PHYSICAL REVIEW D VOLUME 51, NUMBER 6 15 MARCH 1995

Nontrivial dynamics in the early stages of inflation

E. Calzetta* and C. El Hasi†
Instituto de Astronomía y Física del Espacio, Casilla de Correo No. 67, Sucursal 28, 1428 Buenos Aires, Buenos Aires, Argentina
and Departamento de Física, Universidad de Buenos Aires, 1428 Buenos Aires, Buenos Aires, Argentina
(Received 15 August 1994)

Inflationary cosmologies, regarded as dynamical systems, have rather simple asymptotic behavior insofar as the cosmic baldness principle holds. Nevertheless, in the early stages of an inflationary process the dynamical behavior may be very complex. In this paper, we show how even a simple inflationary scenario, based on Linde's "chaotic inflation" proposal, manifests nontrivial dynamical effects such as the breakup of invariant tori, the formation of cantori, and Arnol'd's diffusion. The relevance of such effects is highlighted by the facts that even the occurrence or nonoccurrence of inflation in a given universe is dependent upon them.

PACS number(s): 98.80.Cq, 04.20.Cv, 46.10.+z

I. INTRODUCTION

In this paper, we shall study the behavior of simple inflationary models of the Universe, regarded as dynamical systems. For concreteness, we shall concentrate on models such as Linde's chaotic inflation scenario [1], where inflation is powered by the vacuum energy of a single slowly rolling inflaton field. We shall also restrict ourselves to the actual inflationary period, well before "reheating" starts. As could be expected, we shall find that, once inflation begins, the Universe quickly falls into a de Sitter-like expansion, in agreement with the "cosmic baldness" principle [2]. Nevertheless, we shall also find that extremely complex behavior may occur in the very early stages of inflation, before expansion becomes exponential. The list of nontrivial dynamical effects to be found includes the break up of Kolmogorov-Arnol'd-Moser (KAM) tori [3], the formation of cantori [4], and Arnol'd's diffusion [5]. Indeed, whether or not a given Universe undergoes inflation depends on these effects. Since the complexity of behavior increases with the number of degrees of freedom of the dynamical system, similar conclusions hold for models based on nonminimal inflaton sectors, and indeed for any model based on a second-order phase transition and/or assuming a "slow roll" period [6].

The dynamics of cosmological models, allowing for an inflaton field as the only matter present, has been studied by many authors [7]. In these studies, it is customary to assume homogeneity and isotropy, and a convenient gauge choice; the resulting dynamical system has only two degrees of freedom, e.g., the homogeneous inflaton field amplitude Φ and the Friedmann-Robertson-Walker (FRW) "radius of the Universe," a. The behavior of the system is relatively simple, displaying an inflationary attractor in phase space.

Nevertheless, gravitation and a homogeneous inflaton cannot be the only fields in a workable inflationary model. At some point, the inflationary expansion must "gracefully exit" to a radiation-dominated FRW epoch. This demands that the inflaton field can decay into radiation during the "reheating" era. We do not have the freedom to assume that this radiation field has vanishing amplitude before reheating. The initial conditions for the radiation field, in the classical regime, are decided by the earlier quantum and semiclassical eras.

In fact, simple quantum models of the Universe predict that the radiation field was in its vacuum state at the beginning of the semiclassical era [8]. However, quanta of the radiation field are created subsequently out of the gravitational field itself, much in the same way as gravitational perturbations are generated [9]. While the radiation field would be usually protected against cosmological particle creation by conformal invariance [10], in our case, conformal symmetry is broken by the nonvanishing inflaton vacuum expectation value and the radiation coupling to it. Moreover, conformal symmetry may be broken by other reasons as well; for example, radiation quanta may be created out of the decay of primordial anisotropies [11]. We are therefore led to assume a finite amplitude for the radiation field at the beginning of the classical regime.

Indeed, we must adopt for the radiation field the same "chaotic" view of initial conditions [1] usually applied to the inflaton. This means that matter fields emerge from the semiclassical era, taking uncorrelated values in different patches of the Universe; the dispersion of these values is such that they occasionally approach Planckian scales. Since we are interested in the evolution of a small region of the Universe, though, we can treat the relevant fields as coherent and homogeneous.

In this paper, therefore, we shall focus on the dynamical effects of including a radiation field ψ in an inflation-

*Electronic address: calzetta@iafe.uba.ar
†Electronic address: elhasi@iafe.uba.ar

ary model, in addition to the homogeneous component of the inflaton field. "Radiation" may be described as a conformal scalar field; however, as we already remarked, conformal symmetry is broken by the nonvanishing expectation value of the inflaton, and ψ develops a mass through its coupling to it.

In an earlier communication, we have shown that the dynamical system obtained from coupling a spatially closed, FRW universe to a conformally coupled but massive scalar field displays homoclinic chaos [12,13]. While it would be improper to describe an inflating cosmology as "chaotic," as the typical trajectories are unbounded, it should be clear that the breaking of conformal symmetry results in a definite increase in the complexity of the dynamics. Concretely, while under conformal symmetry there is a sharp separation between inflating and recollapsing universes, once conformal symmetry is broken there appears a full measure stochastic layer in phase space, where orbits may either be trapped forever or escape and approach de Sitter expansion. The reason why recollapse may be avoided, namely, that the action variable associated to the radiation field is no longer conserved, parallels the particle creation processes to be found in semiclassical inflationary models [10], which have a similar, inflation-enhancing effect [11]. Indeed, the above action variable is essentially the particle number of the second-quantized radiation field, as defined by the adiabatic particle model [14].

In this paper we shall consider two different models displaying the influence of a scalar radiation field on the expansion of the Universe in the early stages of inflation. In the first model, the radiation field itself will be considered homogeneous, along with the metric and the inflaton field. In the second model, we shall allow the radiation field to be constituted by a homogeneous background plus an inhomogeneous mode. Of course, the actual presence of such modes is dictated by the dynamics of particle creation. The metric itself will be taken always as that of a spatially closed FRW model, with the "radius of the Universe," a. This assumption, which, in the context of the second model, is inconsistent with Einstein equations, may be justified physically. Indeed, our only concern is to study how the dynamics of the Universe reacts to an increased number of degrees of freedom. From this point of view, the consideration of graviton modes, along with the inhomogeneous scalar field mode, short of posing the full field theoretical problem, would not bring any new qualitative features [15].

It is interesting to observe that taking as canonical variable a gauge-invariant quantity built from scalar and graviton modes [16], rather than the scalar field amplitude itself, would lead to similar results to ours. Indeed, these quantities may be described as scalar fields with time-dependent masses [17].

Let us now describe in more detail the models to be studied. Since the inflaton field, given the "slow roll" assumption, plays no dynamical role in the epoch of interest, we shall replace it with a fundamental cosmological constant Λ (the full evolution of a FRW universe coupled to a minimal, massive scalar field is analyzed in Ref. [18]). The radiation field ψ will be conformally coupled to a, but also have a mass m. The mass $m \sim e\Phi$, where e is the coupling between inflaton and radiation, and Φ the inflaton vacuum expectation value. The "charge" e is bounded by the requirement that the induced inflaton self coupling ($\sim e^4$) should not be too large, and Φ is bounded by the assumptions of slow rollover, enough inflation, etc. This still allows for values as high as $e \sim 10^{-3}$, $\Phi \sim 10^2$ (in natural units, $h = c = 8\pi G = 1$), which gives $m \sim 10^{-1}$ [19].

If the radiation field mass is neglected, we have conformal symmetry and the system is integrable. The metric and the field ψ (from now on "the field") are decoupled, except that the metric reacts to the full field energy density ρ/a^4, $\rho = (1/2)(p_\psi^2 + \psi^2) \equiv$ const. There are two unstable static solutions, the Einstein universes defined by $a = \pm 1/2\sqrt{\Lambda}$, $\rho = 1/16\Lambda$. They are joined by two heteroclinic orbits. Within the separatrix, defined by the heteroclinic orbits, motion is quasiperiodic and confined to invariant KAM tori. Inflating orbits are unbounded, and approach asymptotically the stable and unstable manifolds of the static solutions. Thus, all inflating universes share the same asymptotic behavior, in agreement with the "cosmic baldness" principle.

In the conformally symmetric model, therefore, there is a sharp distinction between inflationary and recollapsing initial conditions. Restricting ourselves to universes arising from a big bang ($a = 0$ at the origin of time), they inflate if $\rho > (16\Lambda)^{-1}$, and recollapse if $\rho < (16\Lambda)^{-1}$. There is no orbit connecting one region to the other, as the separatrix stands as an insurmountable barrier.

When the field develops a mass, it becomes nonlinearly coupled to a. This coupling induces internal resonances between a and ψ, and, consequently, both the separatrix and underlying resonant KAM tori are destroyed. Instead, there arises a new kind of structure in phase space, the stochastic layer [12,13]. The structure of the layer is best analyzed by means of Poincaré sections [20]. It is found that, alongside with fixed points and invariant tori, there is a new kind of invariant orbit, the "cantori" [4]. Cantori have gaps in them, which allow for communication between different parts of the stochastic layer and the outside. The separation between inflating and recollapsing initial conditions becomes less clear-cut: Orbits starting from below the original separatrix may now find their way through the gaps and become inflating, through a process of Hamiltonian diffusion [5]. The occurrence of inflation in a given universe, therefore, may depend upon a nontrivial dynamical effect such as the breakup of KAM tori.

As long as we consider the field ψ as homogeneous, there will be always a critical value of the momentum p_a, such that orbits leaving the singularity from below this threshold are bound to recollapse. This is because the available phase space, once the Hamiltonian constraint is enforced, is three dimensional, and thus it is separated by two-dimensional KAM tori. Therefore, any unbroken torus traps the phase space volume inside it, and makes recollapse unavoidable. Moreover, it should be clear that this critical value will be close to the separatrix value of $p_a \sim 1/\sqrt{8\Lambda}$ at $a = 0$, at least for small field masses. Similarly, while phase volume conservation implies that some

orbits starting from outside the separatrix must enter the stochastic layer and be trapped, it should be clear that the field mass will not greatly affect the behavior of orbits much above the separatrix. From these considerations, it could be concluded that the kinds of effect discussed above are associated with exceptional initial conditions.

However, as we shall show presently, the stochastic layer is localized in phase space because we have assumed a model with only two degrees of freedom. Such localization is not found in higher-dimensional models, such as those allowing for inhomogeneous fields and geometry. The second model to be considered in this paper, adding a single inhomogeneous mode to the homogeneous ψ background, is a first step in the study of those more complex models.

The dynamics of nonintegrable systems in higher dimensions is qualitatively different from that of their two-degrees-of-freedom counterparts. In our case, we have a six-dimensional phase space $(a, \psi, \psi_1, p_a, p_\psi, p_{\psi 1})$, where $(\psi_1, p_{\psi 1})$ stand for the amplitude of the inhomogeneous mode and its canonically conjugated momentum. Even after enforcement of the Hamiltonian constraint, the available phase space is five dimensional, and it is not divided by three-dimensional tori. Thus, unbroken KAM tori do not negate diffusion, and, in principle, a trajectory beginning from $a = 0$, with arbitrarily small $|p_a|$, may nevertheless find its way beyond the separatrix and inflate.

This effect provides a sort of classical mechanism for "creation from nothing" [21]. It makes it unnecessary to assume an unnaturally high value of the initial radiation energy density to explain how the Universe could avoid recollapsing much before inflation had a chance to begin. It recalls previous analyses of semiclassical cosmology, where particle creation has been invoked to satisfy a similar task [11]. It also shows that the nontrivial dynamical behavior discussed here is indeed widespread in phase space.

Our goal in this paper is to point out the manifestation of the nontrivial dynamical effects described above in numerically generated solutions to our models, both the homogeneous and the inhomogeneous, higher-dimensional one. Of course, since Hamiltonian diffusion is such a slow process [22], it would be extremely hard to follow numerically, with proper accuracy, a single diffusing orbit from a neighborhood of the origin in phase space until it becomes definitely inflationary. Instead, we have built Poincaré sections [20] for both models (in the second model, where the Poincaré section would be four dimensional, we shall present only three-dimensional projections of it), and studied the Lyapunov exponents corresponding to selected initial conditions [23].

Poincaré sections are built by selecting a given plane on phase space, and collecting the points where a given orbit crosses this plane in a chosen sense. The full dynamics induces a "return map" on the Poincaré section, both flow and map sharing the same degree of complexity from the standpoint of dynamical systems theory. Thus, for example, the orbits of the map induced by an integrable dynamical system with two-dimensional sections will be either topological circles or else isolated points; an orbit that would not fit in any of these two types is therefore a strong indication of nonintegrability. Poincaré sections are an especially valuable tool in investigating generally covariant dynamical systems, as they convey in a simple fashion information on the dynamics [12,13]. This information concerns the topology of the orbits, which is gauge invariant.

In our case, the simpler, purely homogeneous model has a four-dimensional phase space. We shall choose the $\psi = 0$ plane to build the Poincaré section; since the canonical momentum p_ψ depends on the other variables by the Hamiltonian constraint, the section is two dimensional.

The second model would have four-dimensional sections. For ease of representation, it is desirable to reduce the dimensionality of the section by imposing a second constraint ($\psi_1 = 0$, say) on the selected points. However, this space is populated by points, not by a continuous trajectory; and the probability of a point falling on an arbitrarily chosen surface is zero. Therefore we must take not a true section, but rather a *slice*, allowing the "space of section" to have a finite thickness, in order to catch points [20]. As a matter of fact, in the range covered by our simulations, the shape of the sections is essentially insensitive to ψ_1, and so we have simply left it unspecified. We have found it best to describe the sections in terms of coordinates (a, p_a, j). Here $j = (1/2\omega)p_\psi^2$ ($\omega^2 = 1 + m^2a^2$) is the adiabatically invariant amplitude associated with the homogeneous mode at the zero crossings. Of the two undetermined canonical variables (the amplitude and momentum of the inhomogeneous mode), one can be deduced from the Hamiltonian constraint, and so we are losing only one dimension of the real Poincaré section. As we have verified, this entails no significant loss of information.

Another technique to analyze the higher-dimensional model is to plot, in the space of initial conditions, the region corresponding to orbits that escape the separatrix in less than 500 iterations of the Poincaré section return map. Restricting ourselves to universes with vanishing initial volume and field, and imposing the Hamiltonian constraint, the space of initial conditions is two dimensional; we have chosen the initial values of p_a and p_ψ as suitable coordinates. As befits a chaotic system, the border of the set of inflating trajectories is highly irregular, with thongs of inflating initial conditions penetrating the regular region, and islands of regularity otherwise surrounded by unstable solutions. This plot affords a glimpse of the structure of the Arnol'd web.

A more common tool for the study of nontrivial dynamical systems is the calculation of Lyapunov exponents [24]. These measure the average instability of the orbits of a dynamical system. If the system executes bounded motions, then the Lyapunov exponents may be related to the Kolmogorov-Sinai entropy; in particular, positive Lyapunov's exponents are a sufficient condition for chaos [25]. In our case, this identification does not hold, since most orbits eventually escape the separatrix and inflate; here, the Lyapunov exponent would only relate to the time constant of the inflationary exponential expansion of the Universe, as the cosmic baldness principle asserts

itself.

More relevant to our discussion are, therefore, the Lyapunov exponents as a measure of the average eigenvalues of the linearized evolution operator for suitable initial conditions, over finite parts of the correspondig orbits [23]. Essentially, we shall use Lyapunov exponents to obtain a quantitative measure of the strong sensitivity to initial conditions displayed by the Poincaré sections (see below). Indeed, we shall see how orbits with close initial conditions are characterized by highly different sets of exponents, corroborating the visual information conveyed by the Poincaré sections.

Our numerical simulations will offer concrete examples of all the kinds of nontrivial dynamical behavior discussed above. For the homogeneous mode, we shall see, through the Poincaré sections, the destruction of the conformal KAM tori, their replacement by chains of islands, and the formation of a stochastic sea among the islands. We shall display concrete instances of orbits beginning in the stochastic sea, and eventually leaving the separatrix. This shows that the stochastic sea contains no unbroken tori, but rather it is composed of cantori layers. As a check on our codes, we shall verify the validity of the cosmic baldness principle for inflating orbits.

We shall also display two Poincaré sections of the inhomogeneous model, corresponding one to a stable, regular trajectory and the other one to an unstable one, which eventually becomes inflationary. Comparing these two sections, we shall be able to observe how the destruction of constants of motion is reflected in the topology of the orbit. The pervading strong sensitivity to initial conditions is also reflected by the Lyapunov's exponents associated with each orbit, which we computed.

From the results of these numerical experiments, we shall conclude that a realistic inflationary cosmological model, regarded as a dynamical system, is complex enough to allow for highly nontrivial behavior. Moreover, nonlinearity is a major force in shaping the behavior of the model, even where the cosmic baldness principle holds. A correct understanding of the incidence of these kinds of phenomena may well illuminate several standing issues in inflationary cosmology, which are still oftentimes solved by recourse to fine tuning [26], as well as help us find the proper relationship between classical, semiclassical, and quantum cosmology.

The paper is organized as follows. In the next section we introduce our models, and discuss the main features of the behavior of their solutions, out of simple analytical arguments. In Sec. III, we shall present the results of our numerical simulations. We conclude, in Sec. IV, with a brief discussion of the overall lessons to be learned.

II. MODEL

In this paper, we shall consider spatially closed Friedmann-Robertson-Walker universes coupled to scalar matter and radiation. The metric takes the form $d\sigma^2 = a^2(\eta)(-d\eta^2 + ds^2)$, where η is "conformal time" and ds^2 denotes an invariant metric on the Euclidean three-sphere. The matter field, namely, the "inflaton," will be taken as a real scalar field Φ, minimally coupled to the curvature, with effective potential $V(\Phi)$. "Radiation" shall be described by a massless real scalar field conformally coupled to the curvature. This means that the Lagrangian density shall contain a $(-a^4/12)R(\psi/a)^2$ term, ψ being the conformally scaled scalar field and $R = (6/a^3)(\ddot{a} + a)$ the scalar curvature [we shall follow Misner-Thorne-Wheeler (MTW) conventions throughout [27]; a dot denotes a conformal time derivative]. The inflaton and radiation fields are coupled to each other; this coupling is essential to the "graceful exit" from the inflationary phase.

Insofar as FRW symmetry holds, both scalar fields must be homogeneous. The basic assumption of inflationary cosmologies is that Φ is a slowly evolving field whose effective potential is strictly positive. This positive vacuum energy acts as a cosmological constant, powering an explosive expansion of the Universe ("inflation"). The nonvanishing background value of the inflaton also provides a mass to the radiation field, through Higgs' mechanism. Until the "reheating" phase begins (whereby the inflaton vacuum energy is transformed into radiation energy and dissipated [31]), the inflaton plays no dynamical role and may be taken as constant, its effects being incorporated through the values Λ of the vacuum energy density and m of the radiation field mass. In this regime, the effective degrees of freedom of the model are the "radius of the Universe," a, and the conformally scaled radiation field $\psi(\eta)$. Their conjugated momenta are just their conformal time derivatives $\dot{a} = -p_a$, $\dot{\psi} = p_\psi$. The evolution of these variables in conformal time is described by the Hamiltonian

$$H = \frac{1}{2}[-(p_a^2 + a^2 - 2\Lambda a^4) + (p_\psi^2 + \psi^2) + m^2 a^2 \psi^2], \tag{2.1}$$

supplemented by the Hamiltonian constraint $H = 0$. We shall refer to the system defined by this Hamiltonian as the "homogeneous" model.

The homogeneous radiation field may also be considered as the first term in the expansion of a generic field in terms of three-dimensional spherical harmonics [28]. The different modes are labeled by a positive integer $n \geq 1$; $n = 1$ corresponds to the homogeneous mode. On a FRW background, the higher modes may be described by their conformal time-dependent amplitude and its time derivative. Of course, when the back reaction of these modes is considered, the geometry ceases to belong to the FRW class. However, to obtain a glimpse of the effect of these modes on the cosmic evolution, we may disregard the departure of the metric from its FRW value. For simplicity, moreover, we shall assign a nonzero amplitude to only one mode, say, n_1, with amplitude ψ_1 and conjugated momentum p_1. The Hamiltonian now reads

$$H_1 = \frac{1}{2}[-(p_a^2 + a^2 - 2\Lambda a^4) + (p_\psi^2 + \psi^2) + (p_1^2 + n_1^2 \psi_1^2) + m^2 a^2 (\psi^2 + \psi_1^2)], \tag{2.2}$$

with, as before, the constraint $H_1 = 0$. We shall refer to

this generalization of the model above as the "inhomogeneous" one.

If the effective mass of the radiation field is zero, then geometry and radiation are decoupled, and the resulting dynamics is trivial. When a nonvanishing mass develops, on the other hand, the dynamics of both homogeneous and inhomogeneous models becomes exceedingly complex. Indeed, the dynamics of the $\Lambda = 0$ homogeneous case was studied in detail in Ref. [12], where it is demonstrated how homoclinic chaos arises out of the internal resonances between a and ψ. The $\Lambda \neq 0$ case is briefly considered in Ref. [13]. There it is shown that in the massless case there are two unstable static solutions joined by a separatrix; in the presence of a nonvanishing mass the separatrix is destroyed and homoclinic chaos results. A more detailed analysis based on the structure of fixed points and resonances of the homogeneous model confirms these findings [29].

In view of these results, it should be clear that a thorough investigation of these models requires numerical techniques. However, perturbative arguments, where the effective mass of the radiation field is taken as a small parameter, shed some light on the structure of the solutions and are helpful to understand the numerical results. Therefore, in this section, we shall consider briefly what can be said about these models out of simple perturbative arguments. Later, Sec. III on, we shall consider several numerical experiments, which will disclose the nature of the dynamics without any perturbative assumptions.

Observe that the equations describing our dynamical system remain well defined even upon the cosmic singularities $a = 0$. Thus, a given universe may be analytically continued beyond the singularity, becoming one in a series of cosmic episodes. This series shall extend indefinitely unless, at some link, the trajectory avoids recollapsing and inflates. Therefore, an "orbit" of the recurrence map may actually represent a sequence of many universes. The important point in the present context is not which of these universes inflate and which do not, but rather the fact that some chains, after several recollapsing cycles, actually end with an inflationary episode. This implies a communication between different regions of phase space which would be utterly impossible under an integrable dynamics.

A. Homogeneous model

In this subsection, we shall consider the dynamics generated by the two-degrees-of-freedom Hamiltonian (2.1), constrained to the null energy shell.

In the massless case, we may analyze the evolution of field and geometry independently. The field is just a harmonic oscillator, with unit frequency independent of its amplitude. The radius of the Universe, on the other hand, may be described as an anharmonic oscillator, whose frequency begins as unity, but falls down with amplitude. It actually vanishes as we approach the separatrix connecting the two unstable static solutions. Beyond the separatrix, motion is unbounded, and quickly approaches a de Sitter-like expansion.

Indeed, the frequency of the field oscillations is weakly dependent on amplitude as far as the mass remains small. Therefore, it makes sense to describe the field evolution in terms of the massless action-angle variables j and φ, defined through $\psi = \sqrt{2j}\sin\varphi$, $p_\psi = \sqrt{2j}\cos\varphi$. The Hamiltonian may be split as $H = H^0 + \delta H$, where the integrable, "unperturbed" Hamiltonian $H^0 = -E + j$,

$$E = \frac{1}{2}[p_a^2 + \omega^2 a^2 - 2\Lambda a^4], \tag{2.3}$$

where $\omega^2 = 1 - m^2 j$, while the "perturbation"

$$\delta H = -\frac{1}{2} m^2 j a^2 \cos 2\varphi \ . \tag{2.4}$$

We shall retain the mass correction to the small oscillations frequency, though formally a small term, as this shall improve remarkably the accuracy of our analysis.

It is clearly seen from (2.3) that the properties of the motion depend strongly on whether $m^2 j$ is larger or smaller than unity, in agreement with previous results [12,13]. In the first case, the unperturbed motion is unbounded, and all trajectories correspond to a near–de Sitter inflationary expansion. Therefore, it is in the opposite case $m^2 j < 1$ that we may find nontrivial dynamical effects. This is also the relevant case to investigate the physical question of whether inflation requires greater than Planckian radiation energy densities in the early Universe.

Assuming therefore $m^2 j < 1$, we find that when $E = E_s = \omega^4/16\Lambda$, the "unperturbed" motion admits two static solutions with $a^2 = a_s^2 = \omega^2/4\Lambda$. These solutions are joined by a separatrix. To describe motion below this separatrix, it is convenient to pick E itself as the generalized momentum. Its conjugated variable is, of course, "time," defined as

$$\tau = \int^a \frac{da'}{\sqrt{2E + 2\Lambda a'^4 - \omega^2 a'^2}} \ . \tag{2.5}$$

This definition is easily inverted to yield

$$a = \sqrt{1-\lambda}\, a_s \mathrm{sn}\left[\frac{\omega\tau}{\sqrt{1+k^2}}\right], \tag{2.6}$$

where $\mathrm{sn}u$ denotes the Jacobi elliptic function of the first kind [30], $\lambda = \sqrt{1-(E/E_s)}$ and $k^2 = (1-\lambda)/(1+\lambda)$. We can also Fourier expand a as

$$a = \sqrt{1-\lambda}\, a_s \sum_{n=1} q_n \sin(2n-1)\Omega\tau \ , \tag{2.7}$$

where the Fourier coefficients q_n have standard expressions in terms of complete elliptic integrals [30] and the fundamental frequency

$$\Omega = \frac{\pi}{2\mathbf{K}} \frac{\omega}{\sqrt{1+k^2}} \ . \tag{2.8}$$

Here, $\mathbf{K} = \mathbf{K}[k]$ is the complete elliptic integral of the first kind [30]. We see that $\Omega \to \omega$ when $E \to 0$, and

vanishes when E approaches E_s, as we expected.

Let us observe that, because the transformation from (a, p_a) to (τ, E) depends on j, when the second pair is used, the angle conjugated to j is no longer φ but $\phi = \varphi + \delta\phi$, where

$$\delta\phi = \frac{m^2}{2}\int^{\tau} d\tau'\, a^2(\tau') \ . \tag{2.9}$$

Having solved the unperturbed motion, the analysis follows a standard pattern [13]. The perturbative approach breaks down, and nontrivial dynamics appears, when the oscillations in a become resonant with those in ϕ. Since the leading perturbation goes like $\cos 2\phi$, the leading resonances will be those where $N\Omega = 2$, the unperturbed ϕ frequency being identically 1. This equation has no solution for $N = 1$, and only the trivial one $E = j = 0$ for $N = 2$. Thus the first real breakdown of perturbation theory occurs when $N = 3$. The corresponding KAM torus in the unperturbed dynamics is destroyed by the resonant perturbation, resulting in new homoclinic points and separatrices. These separatrices are further destroyed by other resonant terms, leading to the formation of a stochastic layer. The layers of different resonances tend to overlap with each other, thus forming a stochastic sea extending up to the former separatrix at E_s. Within the stochastic sea KAM tori are replaced by cantori [4], allowing for such phenomena as diffusion; thus an orbit with initial conditions below E_s may escape the separatrix and inflate.

The location of the $N = 3$ resonance is therefore an estimate of the lower limit of the stochastic sea in the full dynamics. It is determined by the resonant condition $\Omega = 2/3$ plus the Hamiltonian constraint $E = j$. For the values $m = 0.65$, $\Lambda = 0.125$, which we shall use in our numerical simulations, the $N = 3$ resonance appears at $E = j = 0.28$. For an orbit starting from $a = 0$, this means that the initial momentum should be $p_a \sim 0.75$. Moreover, it being a $N = 3$ resonance, we expect that a triangular pattern of islands of stability will form in the wake of the destroyed KAM torus in (a, p_a) space.

As we shall see in next section, both predictions of the perturbative analysis are confirmed by the numerical results. For the time being, however, let us turn to the study of the second, "inhomogeneous" model.

B. Inhomogeneous model

In this subsection, we shall apply essentially the same techniques than in the previous one, to the study of the "inhomogeneous" model (2.2). As before, we extend to all phase space the low-amplitude action-angle variables (j, φ) for the "homogeneous" component. For the "inhomogeneous" mode, we write, in the same spirit,

$$\psi_1 = \sqrt{\frac{2j_1}{n_1}}\sin\varphi_1 \ , \tag{2.10}$$

$$p_1 = \sqrt{2n_1 j_1}\cos\varphi_1 \ . \tag{2.11}$$

This allows us to split the Hamiltonian into a perturbation

$$\delta H_1 = -\frac{1}{2}m^2a^2\left(j\cos 2\varphi + \frac{j_1}{n_1}\cos 2\varphi_1\right) \tag{2.12}$$

acting on the unperturbed Hamiltonian $H_1^0 = -E + (j + n_1 j_1)$, where

$$E = \frac{1}{2}[p_a^2 + \omega_1^2 a^2 - 2\Lambda a^4] \tag{2.13}$$

and $\omega_1^2 = 1 - (m^2/n_1)(n_1 j + j_1)$.

The integration of the unperturbed motion may be performed exactly as before. There are two unstable fixed points, at energy $E = E_s^1 = \omega_1^4/16\Lambda$, joined by a separatrix. Above the separatrix, motion is unbounded. To describe the motion below the separatrix, we write $E = E_s^1[4k^2/(1+k^2)^2]$, $0 \le k \le 1$. The evolution of a may be described as a superposition of harmonic oscillations, with fundamental frequency $\Omega_1 = (\pi/2\mathbf{K})(\omega_1/\sqrt{1+k^2})$. Here, as before, $\mathbf{K} = \mathbf{K}[k]$ is the complete elliptic integral of the first kind [30].

As in the "homogeneous" model, it is convenient to choose E itself as canonical momentum. Again this implies introducing a new angle variable τ instead of a, and shifting the angles φ and φ_1 to new angles $\phi = \varphi + \delta\phi$ and $\phi_1 = \varphi_1 + (1/n_1)\delta\phi$. The shift is still given by the expression (2.9), where now of course we must compute the dependence of a on τ using the proper frequency ω_1.

Given the structure of the perturbation, we expect the leading resonances shall be those where the a frequency is a rational multiple of either of the field frequencies. Mode-mode coupling, on the other hand, will only show up at high orders in perturbation theory, and its effects shall be correspondingly weak.

As a matter of fact, the structure of the resonances, as described by the "unperturbed" Hamiltonian H_1^0, is trivial. Since the frequencies are independent of the field amplitudes, they are just vertical lines in the (E, j) plane, accumulating towards $E = E_s^1$. Moreover, since the frequencies belonging to either mode have a fixed, integer ratio, instead of two families of resonances, there is only one. To break this degeneracy, we must consider higher orders in perturbation theory.

To this end, we shall observe that, if we average the perturbation δH_1 over τ, holding ϕ, ϕ_1 fixed, we get the nonzero value

$$\langle\delta H_1\rangle = \frac{\Omega_1}{4\pi}\left\{ j[\sin 2(\phi - \Delta\phi) - \sin 2\phi] + \frac{j_1}{n_1^2}\left[\sin 2(\phi_1 - \frac{1}{n_1}\Delta\phi) - \sin 2\phi_1\right]\right\} \ , \tag{2.14}$$

where $\Delta\phi$ is the accumulated phase shift over one period: namely,

$$\Delta\phi = \frac{m^2\omega_1}{\Lambda}\frac{[\mathbf{K} - \mathbf{E}]}{\sqrt{1+k^2}} \ , \tag{2.15}$$

$\mathbf{E} = \mathbf{E}[k]$ being the complete elliptic integral of the sec-

ond kind [30]. We shall improve our perturbative scheme by introducing this term into the unperturbed Hamiltonian. To perform the actual calculation, however, let us disregard the dependence of ω_1 with respect to j, and j_1; we may, for example, approximate $\omega_1^2 \sim 1 - m^2 E$, which is accurate when $j_1 \sim 0$. This step may not be easily justifiable quantitatively, but it will simplify enormously the analysis below without changing the character of the solutions.

Treating the new term in the Hamiltonian as small, we seek to eliminate it by introducing new action variables x and x_1, where

$$j = \left\{1 - \frac{\Omega_1}{4\pi}[\sin 2(\phi - \Delta\phi) - \sin 2\phi]\right\} x \ , \tag{2.16}$$

$$j_1 = \left\{1 - \frac{\Omega_1}{4\pi n_1^2}\left[\sin 2\left(\phi_1 - \frac{1}{n_1}\Delta\phi\right) - \sin 2\phi_1\right]\right\} x_1 \ . \tag{2.17}$$

This transformation is made canonical by a suitable redefinition of the angle variables, which we do not need to carry through explicitly. Writing the Hamiltonian in terms of the new action variables, and averaging over the old angles, we obtain the new, improved, unperturbed Hamiltonian

$$H_1^1 = -E + \alpha x + n_1 \beta x_1 \ , \tag{2.18}$$

where

$$\alpha = 1 - 2\left(\frac{\Omega_1}{4\pi}\right)^2 \sin^2 \Delta\phi \ , \tag{2.19}$$

$$\beta = 1 - 2\left(\frac{\Omega_1}{4\pi n_1^3}\right)^2 \sin^2 \frac{\Delta\phi}{n_1} \ . \tag{2.20}$$

Observe that $1 - \beta \ll 1 - \alpha$ throughout the energy range, and so there is no significative loss in approximating $\beta \sim 1$.

To obtain the actual form of the resonances, let us solve the Hamiltonian constraint for x_1, obtaining

$$x_1 = \frac{E - \alpha x}{n_1} \ . \tag{2.21}$$

Since x_1 must be positive, we must have $x \leq E/\alpha$.

The equations for the two families of resonances now read as follows.

Case I. $a - \phi$ coupling:

$$x^I = \frac{1}{\alpha'}\left\{1 - \frac{q\alpha}{\Omega_1}\right\} \ , \tag{2.22}$$

where $\alpha' = d\alpha/dE$, and $q < 1$ is a rational number.

Case II. $a - \phi_1$ coupling:

$$x^{II} = \frac{1}{\alpha'}\left\{1 - \frac{q' n_1}{\Omega_1}\right\} \ , \tag{2.23}$$

where $q' < 1/n_1$ is also rational. We see that the two families of resonances have been resolved, although of course the difference in slope between the curves representing each family in the (E, x) plane is much smaller than the slopes themselves. This weak splitting is nevertheless enough to communicate the different resonances among themselves, thus providing the basic pattern of the Arnol'd web.

Another feature of the resonant lines that can be easily checked against the numerical results concerns their overall slope. First, it should be observed that, the denominator in Eqs. (2.22) and (2.23) being generally very small over the physical range, we only obtain the constraint $x \leq E/\alpha$ when the numerator itself is close to zero. Moreover, since Ω_1 is decreasing over the physical range, at zero the numerator will go from positive to negative. For the values $m = 0.65$ and $\Lambda = 0.125$ to be used in Sec. III, the denominator is positive over the range $0.237 \leq E \leq 0.355$. Since x must be positive, we may conclude that the resonant lines have negative slope in this range of energies, reaching the zeros of the numerator from below. In terms of the initial value of the momenta, assuming initially $a, \phi, \phi_1 = 0$, this interval corresponds to $0.688 \leq p_{ai} \leq 0.842$. Of course, a negative dx/dE also implies $dp_{\psi i}/dp_{ai} \leq 0$, in agreement with the numerical results (see below). Outside this range, the resonances should display positive slopes; however, this behavior was not observed, as motion remains regular below the lower limit, and it is too unstable above the upper one.

We shall stop our analysis at this point, proceeding to the presentation of the numerical results.

III. NUMERICAL RESULTS

We now proceed to present the results of the numerical solution of the models described in Sec. II. In these numerical simulations, we have reverted to the original canonical variables $(a, p_a, \psi, p_\psi, \psi_1, p_1)$, whose equations of evolution follow from the Hamiltonians (2.1) and (2.2). The simplicity of these equations makes this approach more appealing than other, more sophisticated alternatives. We have also appealed to the fiction of continuing each solution beyond the cosmic singularities $a = 0$. Therefore, the numerical trajectories to be presented correspond actually to strings of different universes, each being the analytic extension of its parent. This mathematical trick, possible because the equations of motion, as written in the conformal time frame, remain analytical at these singularities, will allow for a more efficient exploration of the dynamics without affecting the physics.

To solve the models, we have used a Runge-Kutta [32] fifth-order routine. This method works well in our examples, mainly due to the particular choice of time variable. We have chosen not to enforce the Hamiltonian constraint, but as a check on the numerical code, surveyed it in all runs, making sure that the value of the

Hamiltonian never exceeded a given threshold of 10^{-10}.

Let us now discuss our results. As in the previous section, we shall begin with the simplest, "homogeneous" model.

A. Homogeneous model

This section is devoted to the study of a homogeneous inflationary cosmological model consistent with a FRW background, an inflaton field, and a conformally coupled scalar radiation field. Because we are interested in dynamical effects during the very beginning of the inflationary stage, we will replace the inflaton field by a cosmological constant Λ, also allowing the radiation field to develop a mass m through Higgs' mechanism. Here and in next section, we assume $\Lambda = 0.125$ and $m = 0.65$, both in natural units. These values are suitable both on theoretical grounds and for the practical implementation of the model; moreover, it can be seen that the general features of the solutions are independent of this particular choice.

Using standard dynamical systems theory techniques the four-dimensional phase space of this model can be reduced to more visualizable two-dimensional Poincaré surface of section. This is built by intersecting a plane ($\psi = 0$, say) with the dynamical flow in the phase space. In this way all the dynamics can be analyzed on, for example, the a-p_a plane. These variables represent the "slow" variables in our problem.

If the conformal symmetry were not broken by the presence of mass, the problem would be integrable and there would be a separatrix sharply dividing the Poincaré section into five regions. One region, around the origin where the motion is bounded, is filled with invariant KAM tori. The other ones correspond to unbounded trajectories that, wheresoever they begin, approach a de Sitter solution. The motion would be regular in all five regions.

Because of the mass term, the separatrix is replaced by a stochastic layer. In this layer the tori, corresponding to the inner region, are broken, being replaced by new structures, cantori and islands of stability. The former are partially broken tori with gaps in them; some trajectories can escape through the gaps, while others remain confined within the stochastic layer. Trapped trajectories also form around the elliptic points left in the wake of resonant tori, and make up the islands of stability.

The five regions on the plane of section are displayed in Fig. 1. The solid lines represent the separatrices connecting the massless unstable static solutions

$$p_a = \pm \frac{1 - 4\Lambda a^2}{\sqrt{8\Lambda}} , \tag{3.1}$$

as well as the other branches of the stable and unstable manifolds emerging from the massless fixed points, which represent inflationary de Sitter solutions. We have also plotted the sections belonging to a few trajectories in the massive case, which manage to escape from the separatrices. It can be easily appreciated that all the orbits approach very rapidly the massless de Sitter solution. This is, of course, just what would be expected from the "cosmic baldness" principle. We can also observe that the separatrices shrink in the presence of mass, as may be expected from the analysis in the previous section.

The fact that some orbits manage to get through a region formerly occupied by KAM tori is a clear indication of the formation of cantori. However, since for small masses the gaps in the cantori are rather narrow, most orbits escape only after a long period of bouncing within the stochastic layer, while others remain bouncing for-

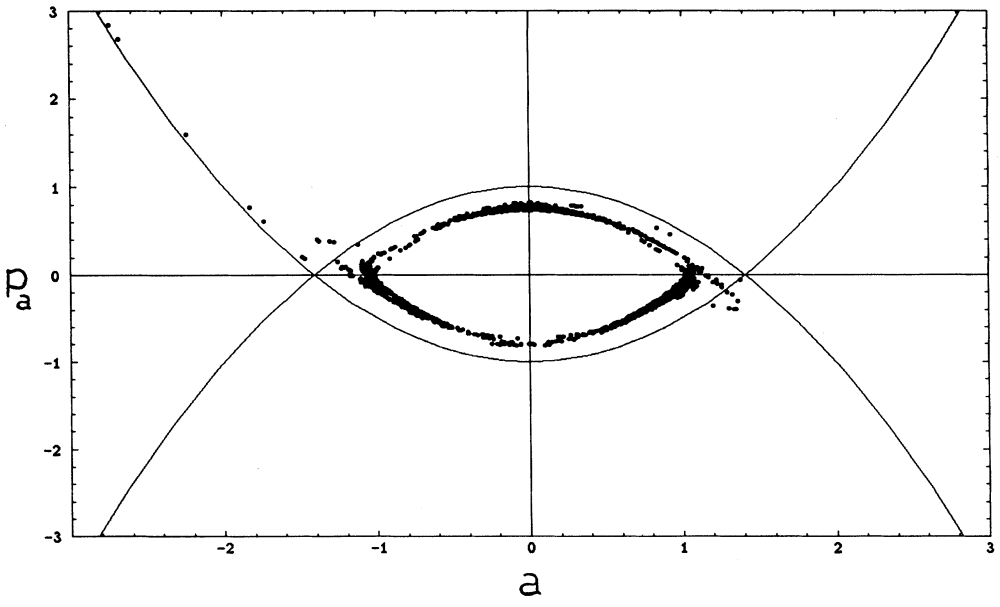

FIG. 1. Poincaré section on the $\psi = 0$ plane. Only the no-boundary trajectories are shown. The solid lines belong to the conformal symmetric case ($m = 0$). Notice the running away trajectories approach the separatrix.

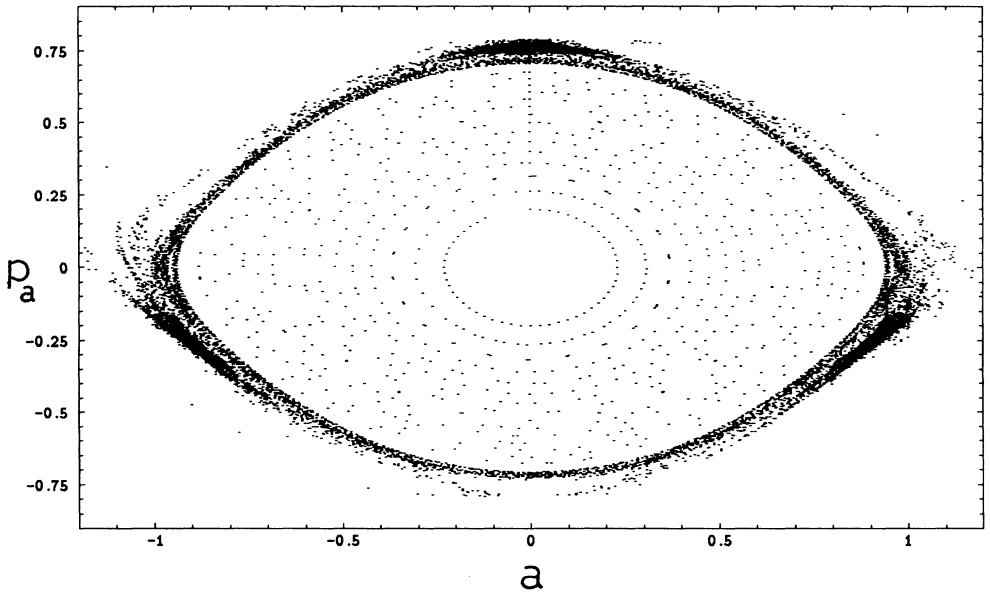

FIG. 2. Same as Fig. 1, including the region of quasiperiodic motion. There are more than 100 trajectories that start at $\psi_i = a_i = 0$, with $p_{\psi i}$ running up to ~ 0.812. The three secondary islands can be appreciated.

ever. Because of Liouville's theorem, another orbits must get in from outside the separatrix, being trapped in the stochastic sea.

The region within the separatrices is shown in greater detail in Fig. 2. This picture corresponds at almost 100 different initial conditions, all of them with $a_i = \psi_i = 0$, but differing in $p_{\psi i}$, which runs up to 0.812. As mandated by the Hamiltonian constraint, $p_{ai} = -p_{\psi i}$. We may appreciate the inner unbroken KAM tori, where the points seem to lie on smooth curves. We note that they are not arranged in sequential order, and so each torus corresponds to several turns around the origin or, in cosmological language, to several cosmic cycles. After those there are several "orbits" corresponding to broken tori, which after several revolutions escape and inflate. Outermost, a new set of stable trajectories makes up a triangular pattern of islands. This chain of secondary islands surrounds the central one in a rather symmetrical way. The slight asymmetry of the two lower islands, due to their relative position with respect to the most likely escape route, can be attributed to the particular choice of initial conditions. It is easily seen that as the mass is increased the last unbroken KAM torus shrinks, but, as long as the field amplitude is different from zero, it never reaches the origin of phase space. The approximate locations of the islands of stability, as well as the triangular pattern, are in excellent agreement with the analysis in the previous section.

In Fig. 3, we exhibit a blowup of the upper island. At the bottom there are several unbroken tori, then a chaotic

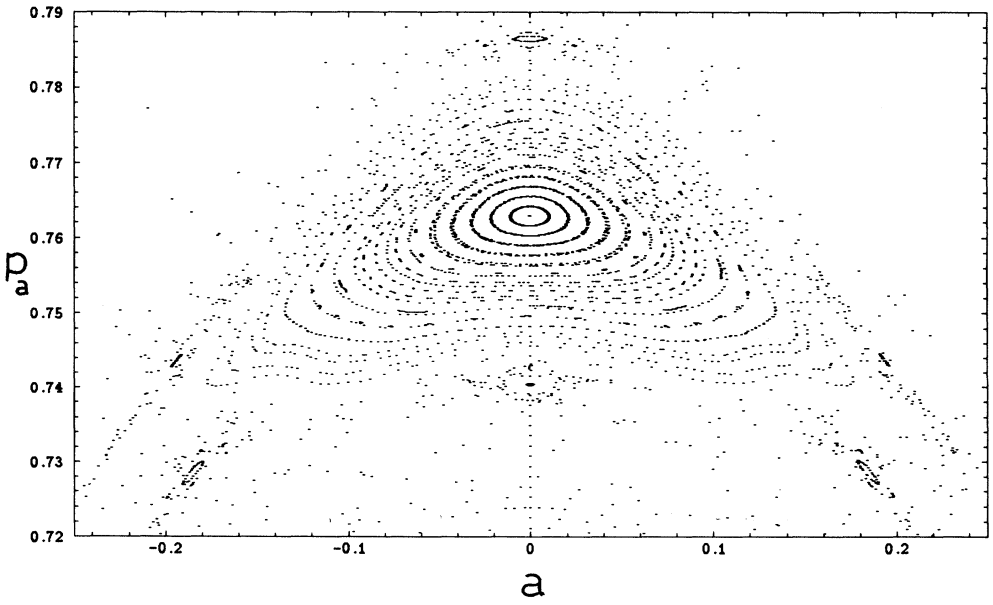

FIG. 3. Blowup of the upper island of Fig. 2. Around this island a similar pattern of third-order islands is clearly seen.

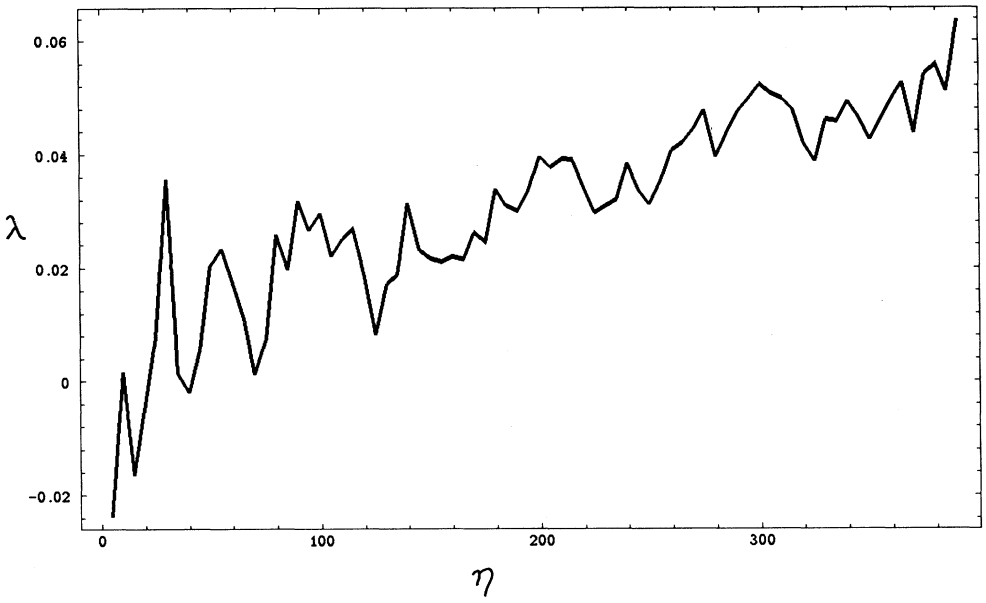

FIG. 4. Maximal Lyapunov exponent for an unstable trajectory (with initial conditions $\psi_i = a_i = 0$ and $p_{\psi i} = 0.736$). It never stabilizes and grows up suddenly when the system escapes away from the separatrix.

or irregular region, and the stable island surrounding an elliptic point on the former KAM torus. As is well known, in nonintegrable systems there exists an infinity hierarchy of such structures, so that around a secondary island there is a pattern of third-order islands, with a fourth-order chain around each, and so on. The radial width of the corresponding island decreases with the order of the chain. This kind of behavior can be clearly appreciated in the picture, where up to third-order islands may be seen. If we were able to get initial conditions close enough to some resonance, it would be possible to go on forever, bringing to light deeper and deeper levels in phase space, until eventually the resolution of the computer is exhausted.

We find that not all the orbits in the chaotic region escape to infinity. Indeed, some of them remain in the stochastic layer for more than 300 iterations of the map, a rather stable behavior. Also, there is no clear-cut divide between stable and unstable trajectories; as we increase the initial momenta, there are unstable orbits following stable ones and vice versa.

As another way to stress the variety of behavior, we have computed the Lyapunov exponents, after the algorithm proposed by Benettin *et al.* and others [23], for a set of different initial conditions corresponding to an unbroken tori, broken tori leading to irregular motion, and stable orbits within the upper secondary island. Figure 4 is a plot of the largest Lyapunov number corresponding to an unstable trajectory with initial conditions $\psi_i = a_i = 0$, $p_{\psi i} = -p_{ai} = 0.736$. After an initial transitory stage, the Lyapunov coefficient becomes positive for several tens of recurrences on the Poincaré section. It never stabilizes, and towards the end it sharply grows, due, most likely, to the unbounded character of this orbit. On the other hand, for initial conditions within the large central island or the secondary ones, the Lyapunov characteristic numbers tend slowly to zero after the initial transitory stage, as expected for regular trajectories. We checked in all cases that, as corresponds to a Hamiltonian system, the sum of the four Lyapunov exponents is zero.

To summarize, this simple model displays extremely complex behavior. The fact that the main features and location of the chaotic region agree with the analysis in Sec. II indicates that these are legitimate effects, rather than numerical constructs. The dynamical effects to be seen include the destruction of KAM tori, and their replacement by cantori and stability islands.

With regards to the cosmological relevance of these findings, it could be objected that they are restricted to a rather special region of phase space. To counter this argument we need to consider the second, "inhomogeneous" model, to which we presently shift our attention.

B. Inhomogeneous model

In this section we shall add a second, inhomogeneous mode to the radiation field. In this way we will be able to analyze the reaction of the system under an increase in the number of degrees of freedom. Indeed, phase space has now six dimensions $(a, p_a, \psi, p_\psi, \psi_1, p_1)$; if we take a section, due to the fixed value of the Hamiltonian, we obtain a four-dimensional Poincaré space of section, which is much more difficult to visualize than the two-dimensional surfaces of section of the previous case.

In an integrable system, there are, besides the Hamiltonian, two other integrals of motion. Therefore the orbits are confined to three-dimensional tori, and their sections can be contained within two-dimensional subsets of the space of section. If the system is perturbed, but we are in a region where the KAM theorem applies, then we also expect two-dimensional sections. At the other extreme, for an ergodic system, points should fill the four-dimensional space of section. Thus, the dimension of the manifold occupied by a sequence of points belonging to

the same orbit can range from 2 to 4.

In our specific model, if the radiation field were massless, the system would be integrable. For example, we could choose as constants of motion in involution the Hamiltonian itself and the field action variables j and j_1, introduced in the previous section. When the mass is turned on, these variables are no longer conserved; however, away from resonances, we expect there will be two other constants of motion, analytic in m^2 and reducing to j, j_1 in the massless limit. Therefore, in the absence of resonances, we expect that the orbits will leave a two-dimensional imprint on a given Poincaré space of section, which we shall choose, by analogy with the previous section, as the $\psi = 0$ plane.

To display this section, however, it is convenient to project it onto ordinary three-dimensional space by constraining also one of the other "fast" variables [33], say, ψ_1. In fact, we have found in our numerical trials that the resulting projection is largely insensitive to the chosen interval in ψ_1; thus, for simplicity, we shall leave ψ_1 unspecified, projecting the actual section onto (a, p_a, p_ψ) space. Of course, in the massless case, the projection lies entirely on a $j =$ const. surface. In the massive case, but in the absence of resonances, there will be an invariant surface close to this plane, which shall contain the orbit. Therefore, the Poincaré section will bend, but it will preserve its shape. On the other hand, upon a resonance, the section will break apart altogether.

To better appreciate this effect, it is convenient to eliminate the adiabatic distortion of the section produced by the evolution of the radius of the Universe, a. To this end, we shall display the numerically obtained sections in (a, p_a, J) space, where

$$J = \frac{\{p_\psi^2 + (1 + m^2 a^2)\psi^2\}}{2\sqrt{1 + m^2 a^2}} \tag{3.2}$$

is an adiabatic invariant. Even with this choice of variables, motion becomes highly irregular as soon as we approach the separatrices. Therefore, we shall confine ourselves to the region in phase space where nonintegrable behavior is first apparent. Also, we shall concentrate on initial conditions where ψ_1 and p_1 are small, since our main concern is to study how the presence of the "inhomogeneous" mode affects the dynamics of a and ψ.

Figure 5 shows a very stable, nonresonant trajectory of our inhomogenous model; it corresponds to more than 1000 recurrences of the orbit on the Poincaré section. The initial conditions for it are $\psi_i = \psi_{1i} = a_i = 0$, $p_{\psi i} = 0.7293$, $p_{ai} = -0.7295$, and $p_{1i} \sim 0.0171$, as given by the Hamiltonian constraint. The trajectory seems to be confined just to a line; although a few points are seen away from the main line of section, they correspond to the late behavior of the simulation, where the loss of stability may be attributed to the accumulation of numerical errors through the simulation. It is also remarkable that the section does not display gaps; we are therefore seeing an unbroken KAM torus, rather than a cantori.

Now, Fig. 6 shows the corresponding picture, for an orbit characterized by the neighboring initial conditions $\psi_i = \psi_{1i} = a_i = 0$, $p_{\psi i} = 0.7293$, $p_{ai} = -0.7294$, and $p_{1i} \sim 0.0121$. This orbit is much less stable than the

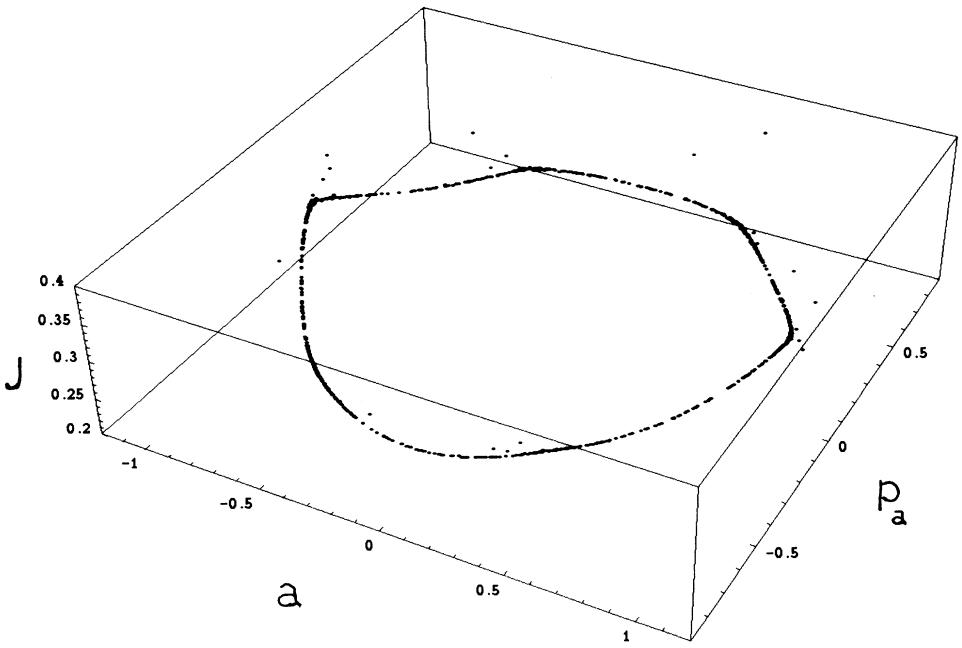

FIG. 5. Poincaré space of section for a stable trajectory (more than 1000 iterations on the section), for the inhomogeneous model. The initial conditions are $\psi_i = \psi_{1i} = a_i = 0$, $p_{\psi i} = 0.7293$, $p_{ai} = -0.7295$, and $p_{1i} \sim 0.0171$, as given by the Hamiltonian constraint.

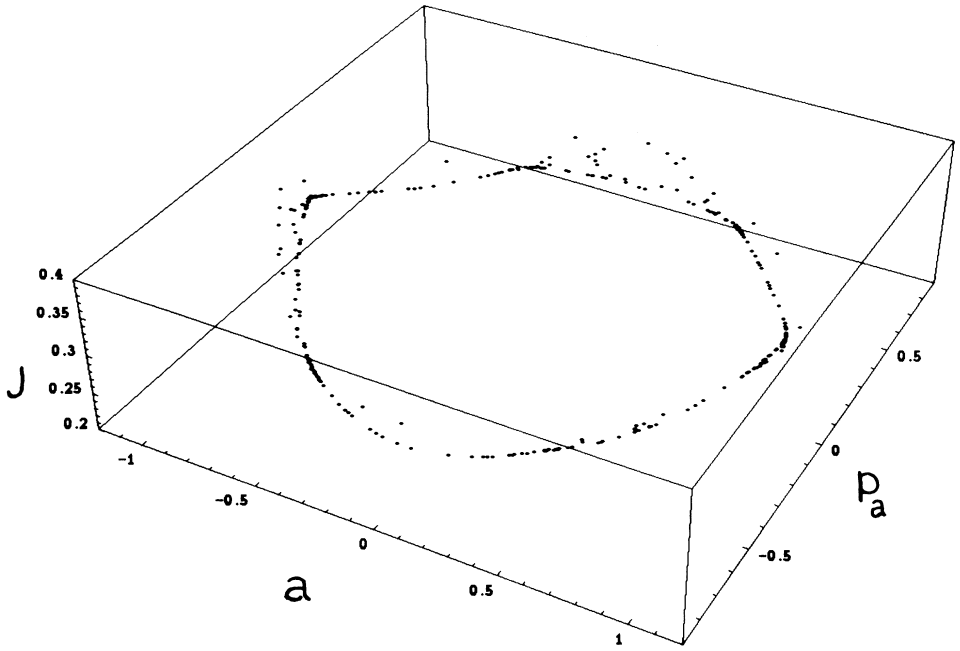

FIG. 6. Same as Fig. 5 for an unstable trajectory. Here the initial conditions are $\psi_i = \psi_{1i} = a_i = 0$, $p_{\psi i} = 0.7293$, $p_{ai} = -0.7294$, and $p_{1i} \sim 0.0121$. Despite the lower value of p_{ai} this is a less regular orbit than the former.

previous one, becoming inflationary after a few hundred iterations of the map. In addition, it is hard to believe that it could fit into a line; it seems to belong to a surface or even a volume. This orbit therefore corresponds to a broken torus. It becomes inflationary by diffusing around the unbroken tori surrounding it, rather than by moving across gaps in them.

To corroborate the results above, Fig. 7 displays a comparison between the Lyapunov exponents associated with each initial condition. The upper one corresponds to the second orbit and its value is around twice the value of the first one. Also in these examples the sum of the Lyapunov exponents remains zero, in good agreement with the Liouville theorem. The first orbit is clearly more stable despite the fact it is closer to the separatrices. It therefore suggests that the unstable orbit is able to somehow find its way around the stable ones, becoming inflationary in spite of the survival of unbroken tori in

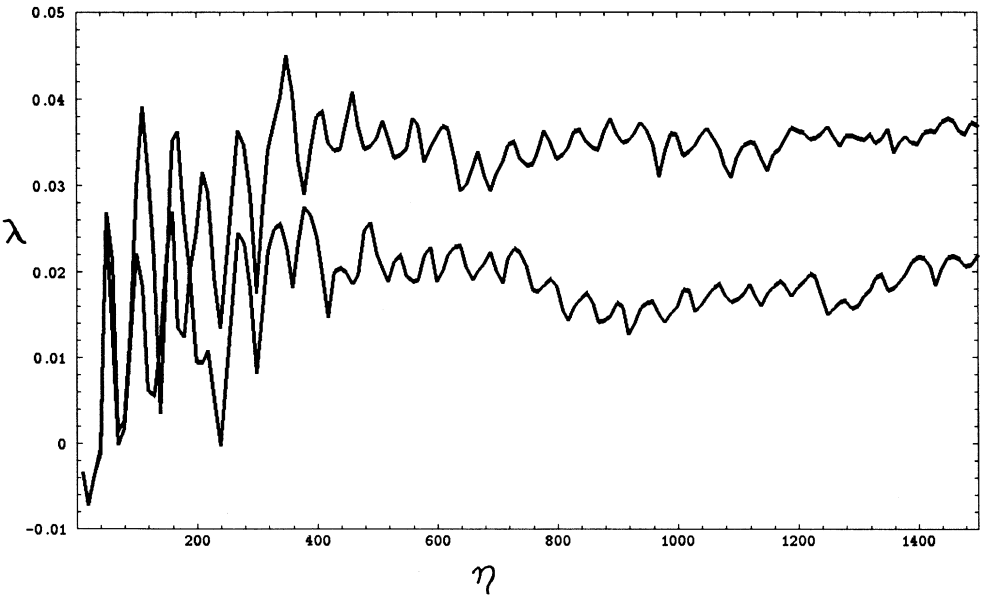

FIG. 7. Comparison between the Lyapunov exponents associated with trajectories shown in Figs. 5 and 6. The upper one corresponds to the second orbit and its value is around twice the value of the first one. The first orbit is clearly more stable despite the fact that it is closer to the separatrix.

the outer layers of the stochastic sea. Indeed, we expect unstable orbits to "diffuse" along the resonant lines of the Arnol'd web. This provides a classical mechanism to achieve inflation starting from fairly generic initial conditions.

Of course, to obtain a direct map of the web is exceedingly difficult [5], since a typical unstable orbit only stays within it a relatively small fraction of the time. Indeed, typical evolution is made of short bursts of fast diffusion along the web, followed by long intervals of seemingly stable motion. There are in the literature rigorous upper bounds for the actual diffusion rates [22]; they are generally exponentially small.

We may obtain an idea of the structure of the web, however, by studying which initial conditions lead to stable (unstable) motion. By constraining ourselves to initial conditions with $a_i = \psi_i = \psi_{1i} = 0$, and enforcing the Hamiltonian constraint, we may reduce these initial conditions to the $(p_{ai}, p_{\psi i})$ plane. Initial conditions close to the web will diffuse more easily and become inflationary faster. Thus, by mapping the regions of instability, we obtain a rough idea of the outline of the web.

In Fig. 8 we display the sector $0.7288 \leq p_{ai} \leq 0.7308$, $0.725 \leq p_{\psi i} \leq 0.73$ in the plane of initial conditions. We have considered initial conditions evenly distributed in this sector, marking with an asterisk those that inflated in less than 500 iterations of the map ("500 ticks of the ψ clock"), and with a dash those that did not. Of course, only initial conditions with $p_{ai} \geq p_{\psi 1}$ are physical; we have removed the lower left and upper right corners, where no structure can be seen.

The map shows clearly the intricate structure of the border of the chaotic region. We can see lines of instability running from upper left to lower right (just as expected from the analysis in Sec. II). Of course, what we are seeing are not just the resonant lines, but the stochastic layers around them. As we progress towards the upper right, these layers merge, and the stochastic sea is formed. Towards the upper left of the figure, where the orbits in Figs. 5 and 6 belong, stable orbits predominate, but it is easy to discern paths connecting unstable initial conditions to the stochastic sea, moving around the stable islands. These are the presumed pathways to inflation.

Figure 9 is a blowup of the central region of Fig. 8. Here, $0.7294 \leq p_{ai} \leq 0.7298$, $0.727 \leq p_{\psi i} \leq 0.728$. We see essentially a similar structure than in the larger plot, which recalls the fractal nature of the actual web. As in the earlier case, the survival of certain islands of stability has no confining effect on deeper unstable orbits.

We can see that not only is the inhomogeneous model more "chaotic" than its homogeneous counterpart, which after all was to be expected, but also the "fine-tuning" objection to the cosmological relevance of chaotic behavior is mostly groundless. In higher-dimensional models, the survival of KAM tori does not confine the deeper layers of phase space, and so essentially all of the phase space is connected to the chaotic region. Quite to the contrary, it is the existence of chaotic diffusion that makes it possible to dispose of the assumption of an unnaturally high radiation energy density to avoid recollapse before inflation. Of course, the addition of semiclassical effects such as particle creation only reinforces this conclusion [11].

To conclude, let us discuss the consistency of having retained the FRW form of the metric in spite of the field being inhomogeneous. We can give a quantitative measure of this inconsistency by computing the contribution from the inhomogeneous mode to the source term in Einstein equations.

Assuming the spatial metric has the form

$$ds^2 = d\chi^2 + \sin^2\chi(d\theta^2 + \sin^2\theta d\phi^2) \ , \tag{3.3}$$

we can expand the scalar field in eigenfunctions of the

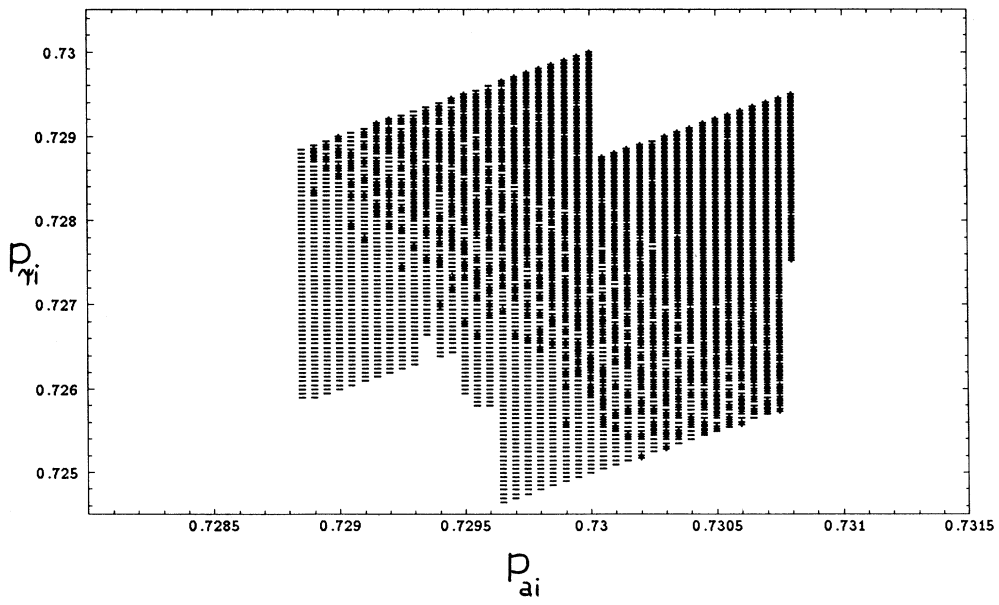

FIG. 8. The sector $0.7288 \leq p_{ai} \leq 0.7308$, $0.725 \leq p_{\psi i} \leq 0.73$ in the plane of initial conditions. Marked with an asterisk are those trajectories that inflated in less than 500 iterations of the map ("500 ticks of the ψ clock"), and with a dash those that did not. Of course, only initial conditions with $p_{ai} \geq p_{\psi i}$ are physical.

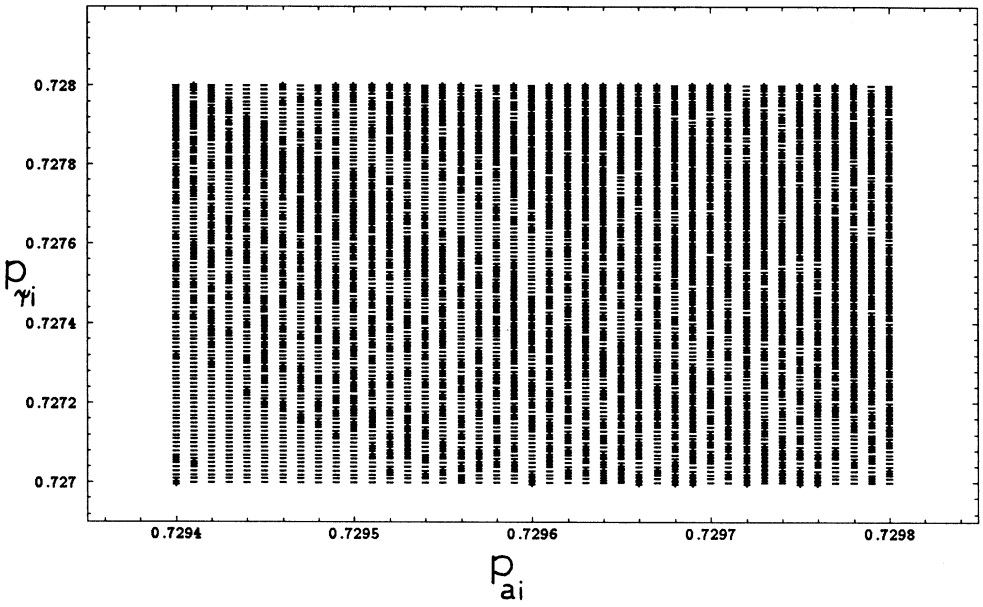

FIG. 9. A blowup of the central region of Fig. 8. Here, $0.7294 \leq p_{ai} \leq 0.7298$, $0.727 \leq p_{\psi i} \leq 0.728$. The structure is essentially the same as in the larger plot, which recalls the fractal nature of the actual web. Also in this case the survival of certain islands of stability has no confining effect on deeper unstable orbits.

three-dimensional Laplacian operator $\nabla^2_{(3)}$ [14]:

$$\Phi(\eta, \mathbf{x}) = \sum_{\mathbf{k}} \frac{\psi(\eta)}{a(\eta)} \mathcal{Y}_{\mathbf{k}}(\mathbf{x}), \tag{3.4}$$

where $\mathbf{x} = (\chi, \theta, \phi)$, $\mathbf{k} = (k, J, M)$ (with $k = 1, 2, \ldots, J = 0, 1, \ldots, k-1$, and $|M| \leq J$), and $\mathcal{Y}_{\mathbf{k}}(\mathbf{x})$ verifying

$$\nabla^2_{(3)} \mathcal{Y}_{\mathbf{k}}(\mathbf{x}) = -(k^2 - 1)\mathcal{Y}_{\mathbf{k}}(\mathbf{x}). \tag{3.5}$$

Just considering the $k = 1, 2$ and $J = 0$ contributions, the scalar field reads

$$\Phi(\eta, \mathbf{x}) = \frac{\psi(\eta) + 2\psi_1(\eta)\cos\chi}{a(\eta)}. \tag{3.6}$$

Substituting Eq. (3.6) into the expression of the stress-energy–momentum tensor for a scalar field [using, for example, Eq. (3.190) of Birrell and Davies [14]], we obtain $T_{00} \equiv \rho$, the energy density of the field. We can estimate the relative weight of the inhomogeneous terms in the source of the Einstein equations from the size of the deviation

$$\sigma^2 = \frac{\langle \rho^2 \rangle - \langle \rho \rangle^2}{\langle \rho \rangle^2},$$

where $\langle \cdots \rangle$ denotes the spatial average.

We have computed σ^2 for the two trajectories shown in this section (Figs. 5 and 6), finding that $\sigma^2 \sim 0.001$. We conclude that the inhomogeneous contribution is around three orders of magnitude smaller than the homogeneous one, and so it may be considered just as a slight perturbation to the FRW metric.

IV. FINAL REMARKS

The main goal of this paper has been to show that even the simplest cosmological models are liable to display highly nontrivial dynamics. This is so even in models such as the ones we have considered here, where the cosmic baldness principle severely limits the asymptotic behavior. The consequences of this behavior for the evolution of the Universe may well be drastic; in the models we have studied, the realization or not of inflation could hinge upon the possibility of chaotic diffusion in phase space.

A second lesson to be learned is the clear difference of behavior between the model with two degrees of freedom and that with three. It should be stressed that from a purely dynamical point of view the addition of the inhomogeneous mode is a rather mild change, since it does not couple directly to the homogeneous mode, and its larger proper frequency shields it from resonances with the "radius of the Universe" (cf. Sec. II). However, the purely topological change brought by the opening of new dimensions in phase space is enough to produce a marked increase in complexity, of which the "deconfinement" of unstable orbits near the origin of phase space is the most conspicuous manifestation.

This indicates that Galerkin- [34] or minisuperspace- [35] type approximations should be used with extreme care, especially when addressing the dynamics of the early Universe, when motions were fast and parametric couplings strong. This word of caution, which has recently came to be accepted by researchers of the quantum era [36], is not less true in classical cosmology.

ACKNOWLEDGMENTS

This work has been partially supported by Fundación Antorchas, CONICET, and UBA (Argentina). We are grateful to David Hobill and Héctor Vucetich for discussing with us an earlier version of this work.

[1] A. D. Linde, Phys. Lett. **129B**, 177 (1983).

[2] G. Gibbons and S. W. Hawking, Phys. Rev. D **15**, 2738 (1977); A. A. Starobinsky, Pis'ma Zh. Eksp. Teor. Fiz. **37**, 55 (1983) [JETP Lett. **37**, 66 (1983)]; K. Nakao, K. Maeda, T. Nakamura, and K. Oohara, Phys. Rev. D **43**, 1788 (1991); **47**, 3194 (1993).

[3] V. I. Arnol'd, Usp. Mat. Nauk. **18**, 13 (1963) [Russ. Math. Sur. **18**, 9 (1963)]; **18**, 91 (1963) [**18**, 85 (1963)]; V. I. Arnol'd, and A. Avez, *Ergodic Problems of Classical Mechanics* (Benjamin, New York, 1968).

[4] I. C. Percival, J. Phys. A **7**, 794 (1974); **12**, L57 (1979); in *Nonlinear Dynamics and the Beam-Beam Interaction*, edited by M. Month and J. Herrera, AIP Conf. Proc. No. 57 (AIP, New York, 1979), p. 302 [reprinted in *Hamiltonian Dynamical Systems*, edited by R. MacKay and J. Meiss (Hilger, Bristol, 1987), p. 367]; A. Katok, in *Dynamical Systems and Chaos*, edited by L. Garrido, Springer Lecture Notes in Physics Vol. 179 (Springer, New York, 1983), p. 47 [reprinted in *Hamiltonian Dynamical Systems*, edited by R. MacKay and J. Meiss (Hilger, Bristol, 1987), p. 376]; S. Aubry, Physica **7D**, 240 (1983) [reprinted in *Hamiltonian Dynamical Systems*, edited by R. MacKay and J. Meiss (Hilger, Bristol, 1987), p. 746]; J. N. Mather, Erg. Theor. Dyn. Syst. **4**, 301 (1984) [reprinted in *Hamiltonian Dynamical Systems*, edited by R. MacKay and J. Meiss (Hilger, Bristol, 1987), p. 395]; R. MacKay, J. Meiss, and I. Percival, Physica **13D**, 55 (1984); J. D. Meiss, Rev. Mod. Phys. **64**, 795 (1992); C. Baesens and R. MacKay, Physica **69D**, 59 (1993).

[5] V. I. Arnol'd, Dokl. Akad. Nauk. SSSR **156**, 9 (1964) [Sov. Math. Dokl. **5**, 581 (1964)]; B. V. Chirikov, Phys. Rep. **52**, 263 (1979); G. M. Zaslavsky, R. Z. Sagdeev, D. A. Usikov, and A. A. Chernikov, *Weak Chaos and Quasi Regular Patterns* (Cambridge University Press, Cambridge, England, 1991); M. A. Lieberman and J. L. Tennyson, in *Long-Time Prediction in Dynamics*, edited by C. W. Horton, L. E. Reichl, and V. G. Szebehely (John Wiley, New York, 1983), p. 179.

[6] F. Lucchin and S. Matarrese, Phys. Rev. D **32**, 1316 (1985); D. La and P. Steinhardt, Phys. Rev. Lett **62**, 376 (1989); F. Accetta and P. Steinhardt, *ibid.* **64**, 2740 (1990); S. Mollerach, S. Matarrese, A. Ortolan, and F. Lucchin, Phys. Rev. D **44**, 1670 (1991); P. J. Steinhardt, Class. Quantum Grav. **10**, S33 (1993); M. Bento, O. Bertolami, P. Moniz, J. Mourão, and P. Sá, *ibid.* **10**, 285 (1993).

[7] V. A. Belinsky, L. P. Grishchuk, I. M. Khalatnikov, and Ya. B. Zel'dovich, Phys. Lett. **155B**, 232 (1985); Zh. Eksp. Teor. Fiz. **89** 346 (1985) [Sov. Phys. JETP **62**, 195 (1985); in *Proceedings of the Third Seminar on Quantum Gravity*, edited by M. A. Markov, V. A. Berezin, and V. P. Frolov (World Scientific, Singapore, 1985), pp. 566–590; S. Gottlober, V. Muller, and A. Starobinsky, Phys. Rev. D **43**, 2510 (1991); L. Amendola, M. Litterio, and F. Occhionero, Int. J. Mod. Phys. A **5**, 3861 (1990); A. Burd, Class. Quantum Grav. **10**, 1495 (1993); G. Abolghasem, A. Burd, A. Coley, and R. van der Hoogen, Phys. Rev. D **48**, 557 (1993); S. Capozziello, F. Ochionero, and L. Amendola, Int. J. Mod. Phys. D **1**, 615 (1993).

[8] J. Halliwell and S. Hawking, Phys. Rev. D **31**, 1777 (1985); S. W. Hawking, in *300 Years of Gravitation*, edited by S. W. Hawking and W. Israel (Cambridge University Press, Cambridge, England, 1987), p. 631; J. J. Halliwell, in *General Relativity and Gravitation 1992*, edited by R. J. Gleiser, C. N. Kozameh, and O. M. Moreschi (Institute of Physics and Physical Society, Bristol, 1993), p. 63.

[9] L. P. Grishchuk, Phys. Rev. D **48**, 3513 (1993); Class. Quantum Grav. **10**, 2449 (1993).

[10] L. Parker, Phys. Rev. Lett. **21**, 562 (1968); Phys. Rev. **183**, 1057 (1969); Phys. Rev. D **3**, 346 (1971).

[11] E. Calzetta, Phys. Rev. D **44**, 3043 (1991).

[12] E. Calzetta and C. El Hasi, Class. Quantum Grav. **10**, 1825 (1993).

[13] E. Calzetta, in *Deterministic Chaos in General Relativity*, edited by A. Burd, A. Coley, and D. Hobill (Plenum, New York, 1994).

[14] N. D. Birrell and P. C. W. Davies, *Quantum Fields on Curved Spaces* (Cambridge University Press, Cambridge, England, 1981).

[15] H. Kurki-Suonio, P. Laguna, and R. Matzner, Phys. Rev. D **48**, 3611 (1993); B. K. Berger and V. Moncrief, *ibid.* **48**, 4676 (1993).

[16] J. M. Bardeen, Phys. Rev. D **22**, 1882 (1980); L. Bombelli, W. Couch, and R. Torrence, Class. Quantum Grav. **11**, 139 (1994).

[17] R. Brandenberger, H. Feldman, V. Mukhanov, and T. Prokopec, in *Origin of Structure in the Universe*, edited by E. Gunzig and P. Nardone (Kluwer, Dordrecht, 1993), p. 13.

[18] R. Laflamme and E. P. S. Shellard, Phys. Rev. D **35**, 2315 (1987); S. W. Hawking, R. Laflamme, and G. W. Lyons, *ibid.* **47**, 5342 (1993).

[19] G. Börner, *The Early Universe*, 2nd ed. (Springer-Verlag, New York, 1992).

[20] M. Hénon, in *Chaotic Behavior of Deterministic Systems*, edited by G. Iooss, R. Hellerman, and R. Stora (North-Holland, Amsterdam, 1983), p. 53.

[21] A. Vilenkin, Phys. Rev. D **27**, 2848 (1983).

[22] N. N. Nekhoroshev, Usp. Mat. Nauk. USSR **32**, 6 (1977) [Russ. Math. Surv. **32**, 1 (1977)].

[23] G. Benettin, L. Galgani, A. Giorgilli and J.-M. Strelcyn, Meccanica **15**, 9 (1980); **15**, 21 (1980); A. Wolf, J. Swift, H. Swinney, and J. Vastano, Physica **16D**, 285 (1985).

[24] V. I. Oseledec, Tr. Mosk. Mat. Obsch. **19**, 179 (1968) [Trans. Mosc. Math. Soc. **19**, 197 (1968)]; H.-D. Meyer, J. Chem. Phys. **84**, 3147 (1986); A. Burd and R. Tavakol, Phys. Rev. D **47**, 5336 (1993).

[25] Ya. B. Pesin, Usp. Mat. Nauk **32**, 55 (1977) [Russ. Math. Surv. **32**, 55 (1977)].

[26] J. E. Lidsey, and R. K. Tavakol, Phys. Lett. B. **309**, 23 (1993); E. Copeland, E. Kolb, A. Liddle, J. Lidsey, Phys. Rev. D **48**, 2529 (1993).

[27] C. Misner, K. Thorne, and A. Wheeler, *Gravitation* (Freeman, San Francisco, 1972).

[28] E. M. Lifshitz and I. M. Khalatnikov, Adv. Phys. **12**, 185 (1963).

[29] S. Blanco, G. Domenech, C. El Hasi, and O. Rosso, Gen. Relat. Gravit. **26**, 1131 (1994).

[30] I. S. Gradshteyn and I. M. Ryzhik, *Table of Integrals, Series, and Products* (Academic Press, New York, 1980).

[31] F. D. Mazzitelli, J. P. Paz, and C. El Hasi, Phys. Rev. D **40**, 955 (1989); J. P. Paz, *ibid.* **42**, 529 (1990); L. Kofman, A. Linde, and A. Starobinsky (unpublished).

[32] W. H. Press, B. P. Flannery, S. A. Teukolsky, and W. T. Vetterling, *Numerical Recipes: The Art of Scientific Computing* (Cambridge University Press, Cam-

bridge, England, 1985).
[33] M. Hénon, in *Chaotic Behavior of Deterministic Systems*, edited by G. Iooss, R. H. G. Helleman, and R. Stora (North-Holland, New York, 1983), p. 53.
[34] A. J. Lichtenberg and M. A. Lieberman, *Regular and Chaotic Dynamics* (Springer-Verlag, New York, 1982).
[35] C. W. Misner, in *Magic without Magic: John Archibald Wheeler*, edited by J. Klauder (Freeman, San Francisco, 1972).
[36] K. V. Kuchař and M. P. Ryan, Phys. Rev. D **40**, 3982 (1989).